Soheila Mahdavi*, Shambhu Kumar Gupta and Mehdi Hojjati

Thermal cycling of composite laminates made of out-of-autoclave materials

https://doi.org/10.1515/secm-2017-0132
Received April 11, 2017; accepted October 25, 2017; previously published online December 12, 2017

Abstract: Carbon fiber-reinforced polymer material has been widely used in space/aerospace industries for manufacturing of spacecraft structures, satellite panels and antennas. In space, composites can be subjected to periodic thermal cycling (TC) in which temperature ranges from –196°C to 180°C, depending on the operational condition. The effect of TC on the properties of flat laminates made of unidirectional (UD) and fabric out-of-autoclave (OOA) material will be presented. Flat laminates were made using the recommended cure cycle by the material supplier. Then, the samples were cut and subjected to the thermal cycle. To do so, the samples were dipped into liquid nitrogen (–196°C) and then transferred to the oven (140°C). After different numbers of cycles (30, 60, 100, 150 and 200), the cross section of the specimens was examined under a microscope for microcrack detection. Other mechanical and physical properties including interlaminar shear strength, storage modulus and coefficient of thermal expansion (CTE) were measured. It was identified that TC can affect the examined properties by two competing factors: (i) more cross-linking in the polymer chain due to post-curing at high temperature during TC and (ii) microcrack formation due to the induced thermal stresses as a result of the matrix/fiber CTE mismatch. It was found that TC can cause microcrack formation and propagation around the voids in the laminate and affect its properties. Depending on the size and shape of the void, microcracks can form at different stages of TC.

Keywords: microcracks; out-of-autoclave composite material; thermal cycling.

***Corresponding author: Soheila Mahdavi,** Concordia Center for Composites, Department of Mechanical and Industrial Engineering, Concordia University, 1455 De Maisonneuve Boulevard W., Montreal, Quebec H3G1M8, Canada, e-mail: soheila.mahdavi@gmail.com
Shambhu Kumar Gupta and Mehdi Hojjati: Concordia Center for Composites, Department of Mechanical and Industrial Engineering, Concordia University, 1455 De Maisonneuve Boulevard W., Montreal, Quebec H3G1M8, Canada

1 Introduction

In the past few decades, fiber-reinforced composite materials have been increasingly used for both structural and non-structural applications. Compared to metallic materials, these composites offer a better combination of strength and modulus, superior strength-to-weight and modulus-to-weight ratios as well as excellent fatigue strength and fatigue damage tolerance. For these reasons, fiber-reinforced composites have been considered for use as substitutes for metal components in many applications in space, aerospace, automotive and sporting goods. Particularly for space applications, such as in spacecrafts and satellites, carbon fiber-laminated composites exhibit high stiffness, low coefficient of thermal expansion (CTE) and good dimensional stability in their lifetimes, which are very important requirements for space material choice [1].

Composite materials in space undergo harsh environmental conditions such as ultraviolet radiation, high vacuum, atomic oxygen, charged particles, man-made debris, micrometeoroids, electromagnetic radiation and thermal cycles, which all cause material degradation. One of the most important environmental effects during the life of a satellite antenna is thermal cycling, in which a composite undergoes a significant temperature change ranging from –160°C to +125°C [2, 3]. When a composite material is exposed to extreme temperature variation, thermal stresses are induced. Thermal stresses are due to the large difference in the CTE of fiber and matrix. Continuous thermal cycles can cause microcrack formation, which leads to fiber/matrix debonding in the composite and, finally, material system failure. Particularly, the mechanical and thermal performance of composites exposed to such thermal cycles has drawn much attention from research communities and space industries [4–8].

There have been several investigations on the effect of thermal cycling on the performance of composites. One of the important criteria concerning the thermal cycling effect on composites is crack development as a function of the number of cycles. Herakovich and Hyer [9] examined the formation of microcracks as a function of the number of thermal cycles on the cross-ply graphite/epoxy composites. They found that the microcrack density increases by increasing the number of thermal cycles,

reaching saturation after a certain number of cycles. Moreover, the presence of transverse cracks significantly reduced the laminate CTE. Henaff-Gardin et al. [10] also observed this saturation phenomenon in carbon/epoxy laminates exposed to thermal cycles from −50°C to 150°C. In another research conducted by Adams et al. [11], the effect of thermal cycling on cross-ply graphite epoxy laminates with different stacking sequences was investigated. Even though the crack density in all the different laminate configurations increased with increasing thermal cycles, it was found that laminate configuration has a significant effect on the crack density as well as the temperature at which transverse cracking initiates. Based on some research works conducted by Bechel et al. [12–14], outer plies in laminates are more susceptible to damage than inner plies.

Han et al. [4] studied the effects of thermal cycling on the mechanical and physical properties of carbon/epoxy composites. Samples were thermal cycled for up to 200 cycles in a temperature range of –196°C to +130°C, and variations in mechanical properties including longitudinal tensile property, flexural property and interlaminar shear strength (ILSS) were measured. They concluded that the material cure was not complete so the heating effect of the thermal cycling caused more cross-linking of the resin matrix, which led to a higher glass transition temperature (T_g). After improving the cross-linking, further cycling caused microcrack formation due to the CTE mismatch between the fibers and the matrix. Increased backbone flexibility caused an increase in microcrack density and decreased the glass transition temperature of the laminates studied. Several other researchers [5, 15] studied the effect of thermal cycling on the T_g and observed the same results.

An attempt to emulate the effect of a space environment on carbon/epoxy specimens was made by Kessler et al. [16]. Test samples were subjected to thermal cycles between –250°C and +125°C. No significant change was observed in material tensile strength after 10 thermal cycles. Thermal cycling of carbon/cyanate ester prepregs was studied by Ajaja and Barthelat [17] to examine the effect of microscopic damage on mechanical properties. Samples were exposed to thermal cycling in two different ways: the first method was extreme cycling in which samples were exposed to cold cycling by dipping quickly in liquid nitrogen (LN; –210°C) and then transferred to room temperature (RT) water (+20°C). In the second method, thermal cycling between +20°C and –120°C was performed in a dynamic mechanical analysis (DMA) with a controlled temperature rate. Almost 50% reduction in bending stiffness was reported after only five extreme cycles, and the microcracks were detected too. However, the bending stiffness of the samples cycled in the DMA did not change even after eight cycles, and no microcrack was observed. The effect of thermal cycling on the CTE of composites was investigated, and no variation was observed, which is in agreement with the results reported by Tompkins [18].

The manufacturing method is an influential factor in composite material properties. Composite structures are often cured in an autoclave to achieve the required space-grade quality. However, curing large structures needs access to large autoclaves, which is limited and expensive. So, fabrication of large structures using out-of-autoclave (OOA) prepreg materials will result in a huge amount of savings in manufacturing costs [19]. In the OOA manufacturing method, the presence of voids has been an issue due to the lack of high pressure onto the laminate to eliminate the voids. As an alternative, a vacuum pump is utilized to exert a low pressure for minimizing the void content [20]. Many researchers have compared OOA prepregs with autoclave materials and found that the properties of the laminates fabricated with the OOA prepregs can be the same as those fabricated with autoclave prepregs [21, 22]. Cauberghs [23] studied the OOA manufacturing of aerospace representative parts with complex shape using carbon/epoxy prepreg technology and compared them with autoclave parts. The mechanical performance of the OOA prepregs, including compression and bending properties, was comparable to that of the autoclave prepregs, and both techniques yielded to void-free parts. Achieving uniformity of the thickness in tight corners was reported to be challenging for both techniques. Therefore, the purpose of this research work was to study the mechanical and thermal properties of the OOA carbon fiber epoxy composite after thermal cycling.

2 Materials and methods

2.1 Materials selection

The material used for this project was CYCOM 5320-1 manufactured by Cytec Engineered Materials Inc. (Tempe, AZ, USA), which is a composite material system for manufacturing primary structural parts in today's aerospace industry. It is a toughened epoxy prepreg system specifically designed for OOA manufacturing. Two different styled composites made up of this material were used for the analysis: a unidirectional (UD) composite and a woven fabric (5-harness carbon/epoxy satin prepreg or

5HS). The purpose of selecting two different styled composites was to examine and compare their mechanical and thermal performance after being exposed to thermal cycling. The samples were manufactured from the same resin system provided by Cytec and had the same total laminate thickness of ~3.5 mm to have results that are comparable.

2.2 Manufacturing of the OOA sample

Two different laminates were made: (1) a UD laminate made of 24 layers of UD prepreg and (2) a cross-ply laminate made of eight layers of 5HS woven fabric (5-harness satin prepregs). The plate was manufactured by the hand layup method and was vacuumed at a level of 20 Torr for 1 h to eliminate the entrapped air and moisture. To track the plate temperature during the curing process and afterward during the thermal cycling process, a k-type thermocouple was bonded to the edge of the midplane of the laminate. Because the carbon fibers are conductive and by touching the thermocouple can cause false temperature reading, a release film was utilized to avoid the contact between the prepreg and the thermocouple wire.

The cure cycle recommended by the manufacturer of the CYCOM 5320-1 material system was used to cure the composite laminates [24]. The material was cured in a forced air circulation oven. A vacuum pump was used to pull the vacuum inside the layup bag. In order to measure more accurately the laminate temperature during the cure and avoid the temperature delay between the oven temperature and the plate temperature, the other end of the thermocouple already embedded in the laminate midplane was taken out of the oven and used for a data acquisition system. It was assumed that once the center ply of the laminate was within ±5°C of the desired temperature, all plies of the laminate had reached temperature equilibrium. The oven temperature was ramped from RT to 120°C and held at this temperature for 3 h to cure the epoxy. Then, it was raised to 177°C and kept for 2 h for post-curing, and finally the plate was allowed to cool down to RT. All the temperature changes occurred at a ramp rate of 0.6–2.8°C/min. One fabric plate and two UD plates were fabricated for this study.

2.3 Thermal cycling

Cycling of the coupon samples was performed in a jar containing LN for the cooling phase and inside a convection oven for the heating phase. The specimens were placed in a basket made of metal wire mesh having different shelves to minimize the contact between them and to make the specimen temperature equilibrium faster. The basket was immersed in the LN bath for the cooling phase and placed in the preheated convection oven for the heating phase of the cycle. After each cooling and heating phase, the basket containing the specimens was placed on the table at the room to reach ambient temperature.

To have a control specimen for thermal cycling, one sample was cut from the laminate such that the thermocouple embedded in the laminate during the manufacturing step was inside the cut sample. The time necessary for the center ply of this control specimen to reach the required hold temperatures (within ±5°C of the target temperature) was recorded for each step of the thermal cycle. A complete cycle was defined as 2 min in the LN at –196°C, 5 min at RT of +23°C, 10 min inside the oven at +140°C, and 5 min again at RT. Thus, the total time for one cycle was 22 min. Five different sets of samples were cycled at 30, 60, 100, 150 and 200 times and were compared with one set of unexposed samples (non-cycled).

3 Experimental results

3.1 Degree of cure

To find out the degree of cure of the laminates, differential scanning calorimetry (DSC) was used. The heat flow of the raw prepreg and cured laminates was measured using a TA Instrument Q200 DSC machine. A temperature ramp from 25°C to 300°C at 10°C/min was run to obtain the total heat of reaction of the raw prepregs and cured laminates. The degree of cure (α) can be calculated using the formula below:

$$\alpha = \left(1 - \frac{\text{residual heat}}{\text{total heat of reaction}}\right) \times 100$$

Five samples were cut from different areas of the laminates in order to have an average representative of the whole plate. The weight of all the specimens was around 10 mg. Based on the data obtained from the DSC graphs, the average degree of cure for the UD laminate was 92% [standard deviation (SD) = 2%] and for the cross-ply fabric laminate was 97% (SD = 1.5%), which indicate a good curing process.

3.2 Microcrack observation

An optical microscope with ×20 magnification was utilized to observe the effect of thermal cycling on the ply-level microcrack initiation and propagation. To do so, one specimen from each laminate prior to cycling was cut and polished on one side of the cross section such that the fibers were perpendicular to the polished edge. Polished samples were examined under a microscope prior to cycling. No visible microcrack was observed. However, there were some voids in the samples due to the OOA curing of the material and the absence of oven pressure during the cure. Then, the samples were taken for microscopy after a specific number of thermal cycles. For the purpose of crack investigation, some samples were analyzed every 1 cycle to check the crack initiation and propagation during the first 10 cycles, and afterward they were analyzed every 10 cycles. As can be seen in Figure 1, for the UD samples, microcracks become more visible after 350 thermal cycles. Cracks started to form by connecting the adjacent voids together and causing delamination cracks between the layers (left inset). A few cracks were also formed within a single ply by joining the voids. All the cracks observed were horizontal, and no vertical cracks (through the thickness) were found through the entire laminate.

The results of the microscopy for the cross-ply fabric are shown in Figure 2 for the first five cycles and in Figure 3 for cycles 10–40. Unlike the UD samples where there was no visible crack up to 350 thermal cycles, imaging of the cross-ply specimen demonstrates the presence of several microcracks in the early cycles. Several cracks were detected at the edges and also around the voids. Figure 2 demonstrates the effect of a large void between the tows in microcrack formation. There was no crack up to four cycles, and then a crack was initiated around the void after the fifth cycle. As shown in Figure 2, another source of crack initiation was observed where the microcrack starts from the surface just after one cycle and propagated until it reached the 0° fibers. Figure 3 shows the crack formation around the voids inside the tows and resin-rich areas (with possible microvoids within). The void sizes are smaller, and it takes more thermal cycling for crack initiation and propagation. All the detected cracks started to grow through the thickness. By increasing the number of thermal cycles, cracks propagated through the whole thickness of the ply and stopped upon reaching the 0° plies.

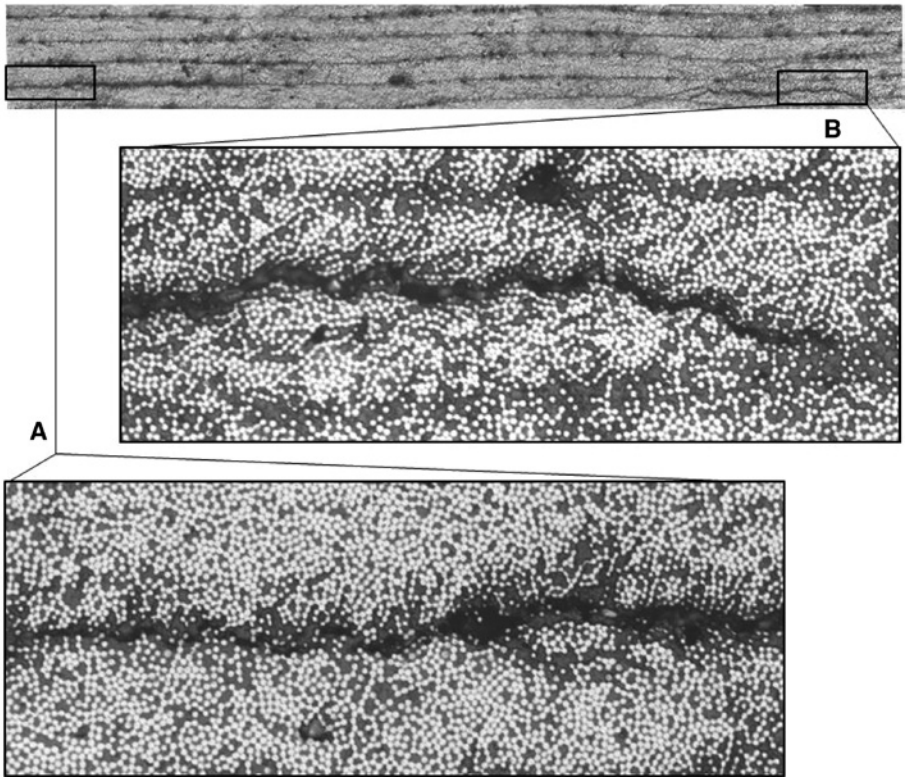

Figure 1: Two optical microscopy images of the UD laminate. Adjacent voids were connected to form horizontal defects (with microcracks) between two plies (A, inset) and also to delaminate the composite within a single ply (B, inset).

3.3 ILSS

The ILSS was measured using an MTS universal testing machine at 22°C and 50% relative humidity, in accordance with the ASTM D2344-13 standard test method. Each data point indicated in the results is an average of five separate specimens with dimensions of 20 mm × 6.5 mm × 3 mm. All specimens were tested using a support span of 14 mm at a crosshead speed of 1 mm/min. The UD specimen broke at maximum load of 2789 N followed by a sharp load drop due to interlaminar shear failure. The calculated ILSS for UD is 99.21 MPa. The maximum load that the cross-ply fabric specimen carried was 1711 N, and then the load dropped due to interlaminar shear failure at midplane. The ILSS for the cross-ply fabric is 63.39 MPa, which is about 36% less than the ILSS of the UD laminate. This is related to the fabric structure as well as the void contents, which is higher in the fabric cross-ply laminates as shown in Figures 1 and 2.

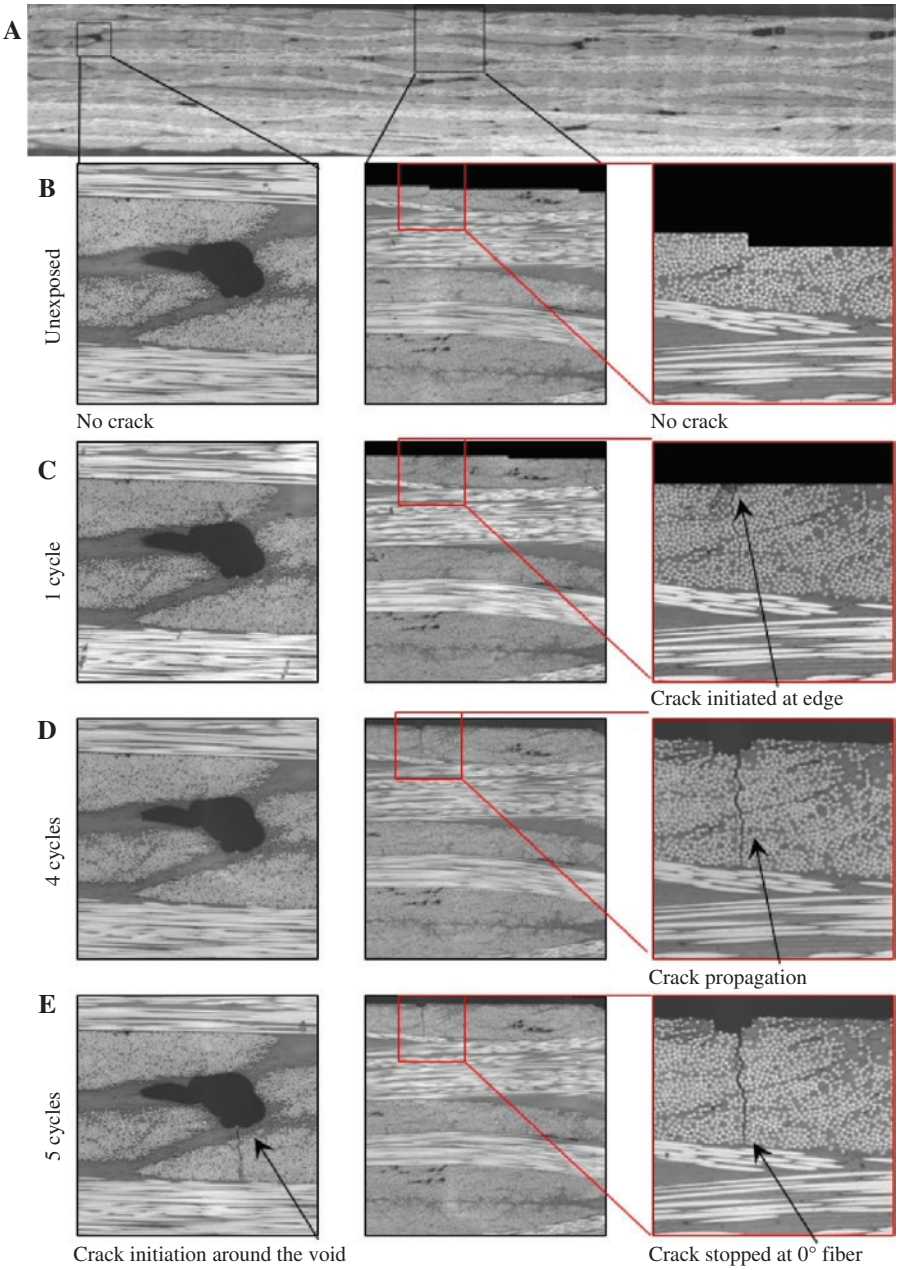

Figure 2: The results of the microscopy for the cross-ply fabric for the first five cycles. (A) Optical microscopy image of the cross-ply fabric laminate; (B) before exposure to thermal cycle; (C) after one cycle; (D) after four cycles; (E) after five cycles. Crack imitation and propagation around the void and close to edge are demonstrated.

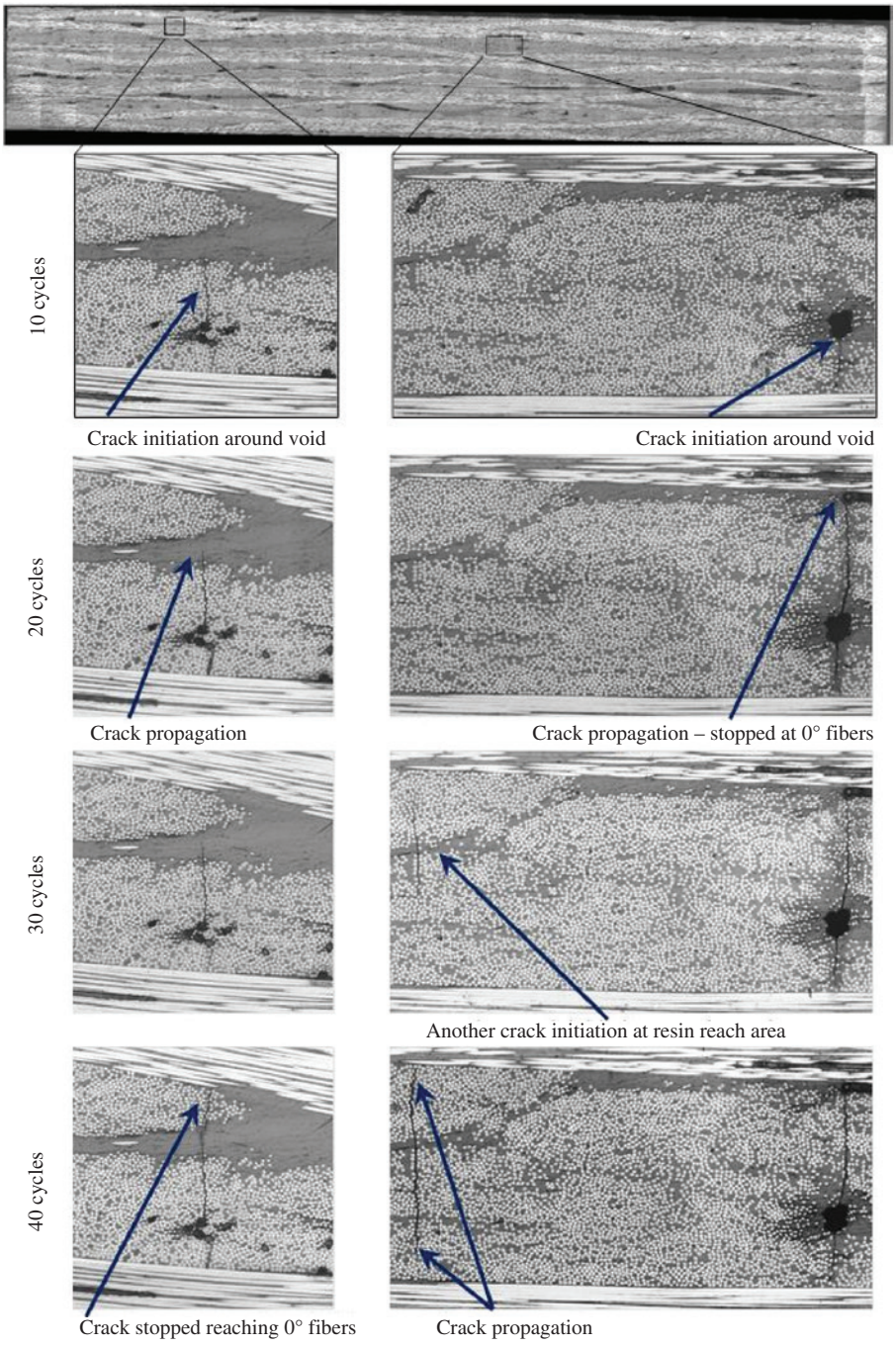

Figure 3: Optical microscopy image of the cross-ply fabric laminate after several thermal cycles. Crack imitation and propagation around the void within tows and at resin-rich areas are demonstrated after 10, 20, 30 and 40 thermal cycles.

Figure 4 shows the variation of the ILSS of the present carbon/epoxy composites versus the different thermal cycles. The values documented are the average of five specimens. The ILSS of the UD composite first gradually decreased until 100 cycles by 8.32% from 99.21 MPa for the unexposed sample to 90.96 MPa. Afterward, it increased by about 11.27% with further cycling to 101.21 MPa for 200 cycles, which is about 2% higher than the unexposed one. The same trend was reported already by Gao et al. [25]. Also, for the cross-ply fabric samples with increasing number of thermal cycles from 0 to 200, the ILSS of the composites gradually decreased by 9.6% from 63.39 MPa for the unexposed sample to 57.31 MPa for the 200-times-cycled sample.

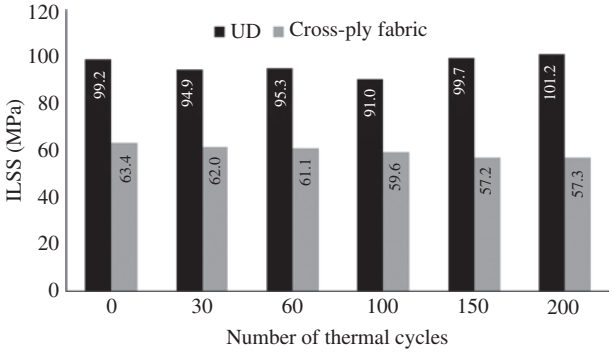

Figure 4: ILSS of the UD and cross-ply fabric composites subjected to different thermal cycles.

3.4 Elastic and viscoelastic properties

The DMA using the TA instrument Q800 was conducted to examine the variation of storage modulus (E'), tan δ and glass transition temperature T_g of the samples after being exposed to thermal cycling and compared with the unexposed samples. The specimens with dimensions of 50 mm × 15 mm × 3 mm were used for the analysis. The analyses were done in three-point bending mode at a frequency of 1 Hz. The samples were heated from –150°C to 320°C at a heating rate of 5°C/min, with 0.05-mm maximum displacement. The T_g was determined from the peak of the tan δ curve. Because the modulus of the carbon fiber was not changing in the temperature range studied in this research, the variations of loss and storage modulus represent the variations in the polymer and/or polymer/fiber interface [26]. The reported results of the DMA are based on the average value of two specimens.

3.4.1 Thermal cycling effect on storage modulus

Figure 5 shows the effect of thermal cycling on the storage modulus of both the cross-ply fabric and the UD laminate in the 90° direction. As the number of thermal cycles increases, the storage modulus of the UD samples decreases with the same trend despite some minor fluctuations in between. As a result of exposure to thermal cycles, by the increase in the number of thermal cycles up to 350 cycles, the storage modulus of the UD composites decreases at extreme low (–150°C) and room (+25°C) temperature by about 8% and 3%, respectively. On the other hand, the storage modulus of the cross-ply fabric samples tends to significantly decrease as the number of thermal cycles increases. At an extreme low temperature of –150°C, the storage modulus reduces from 52.1 GPa for the unexposed sample compared to 39.1 GPa for the 200-times-cycled sample, which is equivalent to 25% reduction in storage modulus as a result of thermal cycling. This reduction for RT is about 19% from $E'_{\text{unexposed}} = 44.3$ GPa to $E'_{\text{200-cycles}} = 36.0$ GPa.

3.4.2 Thermal cycling effect on tan δ

Tan δ is the ratio of loss to storage modulus. Figure 6 shows the variation of tan δ of the laminates subjected to different thermal cycles. For the first 150 thermal cycles, the tan δ of the UD laminate exhibited some fluctuation of less than 6% with respect to the unexposed samples. Then, by increasing the number of thermal cycles from 150 to 200 cycles, it suddenly decreased by ~19% and stayed almost constant with further cycling to 350. It can be seen that the peak of tan δ of the cross-ply laminate

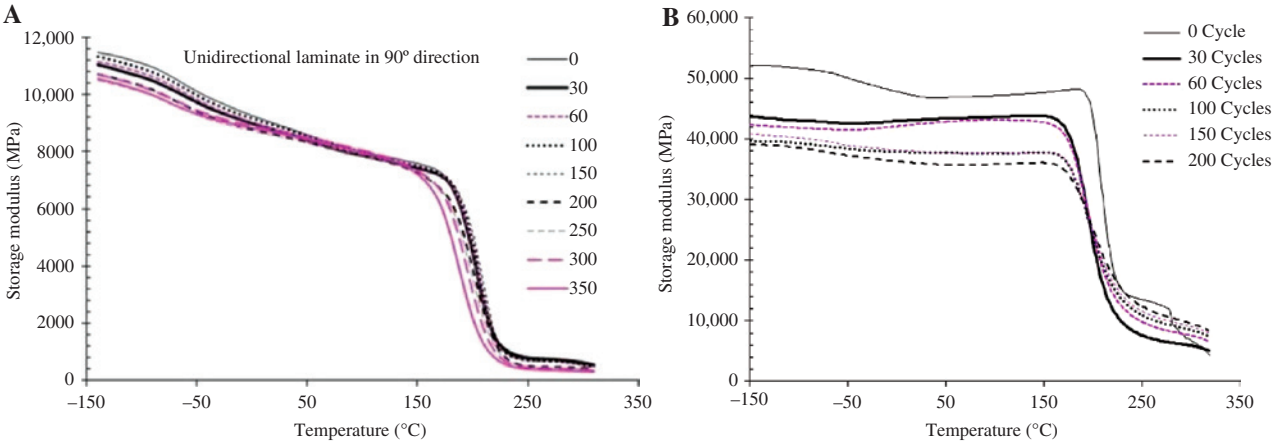

Figure 5: Effect of thermal cycling on the storage modulus of (A) UD and (B) cross-ply fabric composites in the 90° direction.

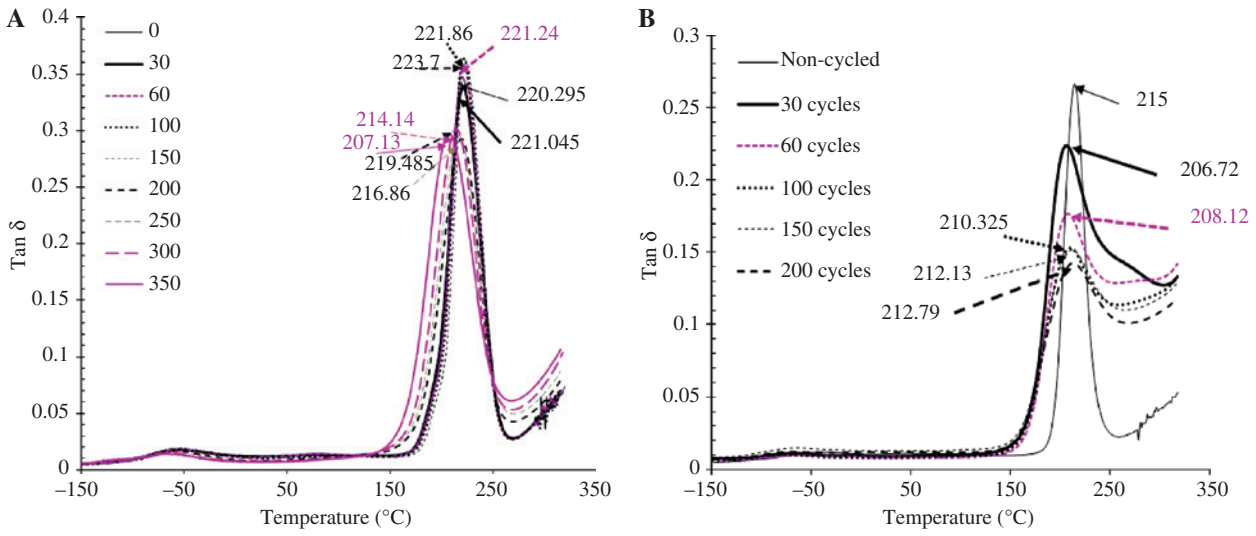

Figure 6: Effect of thermal cycling on tan δ and T_g of (A) UD and (B) cross-ply fabric composites in the 90° direction.

decreases continuously by increasing the number of thermal cycles, but the reduction rate is not the same for all cycles. For the first 100 cycles, tan δ decreases by an average rate of 16%, and afterward it slows down. The reduction of tan δ was 46% from 0 to 200 thermal cycles. It is clear from the curves that by increasing the thermal cycles, the peak values decrease while the curve broadens. The same behavior was observed for the UD laminates, but not as evident as that for the cross-ply fabric laminate. This indicates that stiffness increased while viscosity decreased, which probably is due to the decreased mobility of the molecular chain. Because the polymer was under thermal cycling at high temperature close to its T_g, additional cross-linking and post-curing occurred, which consequently caused an increase in T_g [27].

3.4.3 Thermal cycling effect on T_g

Glass transition temperature T_g can be found from the curves of storage modulus, and tan δ versus temperature in a DMA analysis; however, it is often preferred and more accurate to locate T_g from the peak of tan δ. The value of T_g is marked in the peak of tan δ in Figure 6. For a better comparison, the variation of T_g versus cycles is shown in Figure 7. At the beginning of the thermal cycles, the T_g of the UD composite samples tends to continuously rise up by 1.6% from 220.3°C of the unexposed sample to 223.7°C at 150 cycles. Then, it decreases by 7.4% with further cycling to 207.1°C at 350 cycles, which is about 6% lower than the T_g of the unexposed sample. This trend indicates that during thermal cycling, the rising of the temperature can cause a higher degree of cross-linking of the resin matrix, which consequently induces post-curing to some extent. Further cross-linking causes an increase of T_g. However, this trend disappears after 150 cycles as reported by other researchers [4, 17, 19]. Unlike the UD laminate, the T_g of the cross-ply fabric laminates drops right after 30 cycles by 3.6% from 214.8°C to 207.1°C and then tends to go up again to 212.79°C after 200 cycles.

3.4.4 CTE

The measurements of the transverse CTE were performed using a thermomechanical analyzer, TA instrument Q400, using an expansion probe with flat tip. The machine was operated in standard mode, in which the tip applies a constant static load of 0.08 N while the sample is subjected to

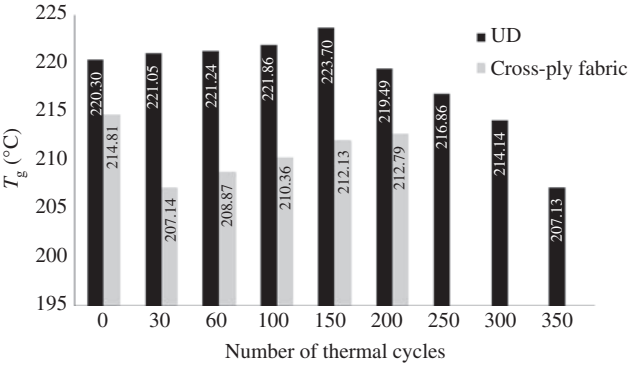

Figure 7: Variation of the T_g of laminates versus the number of thermal cycles.

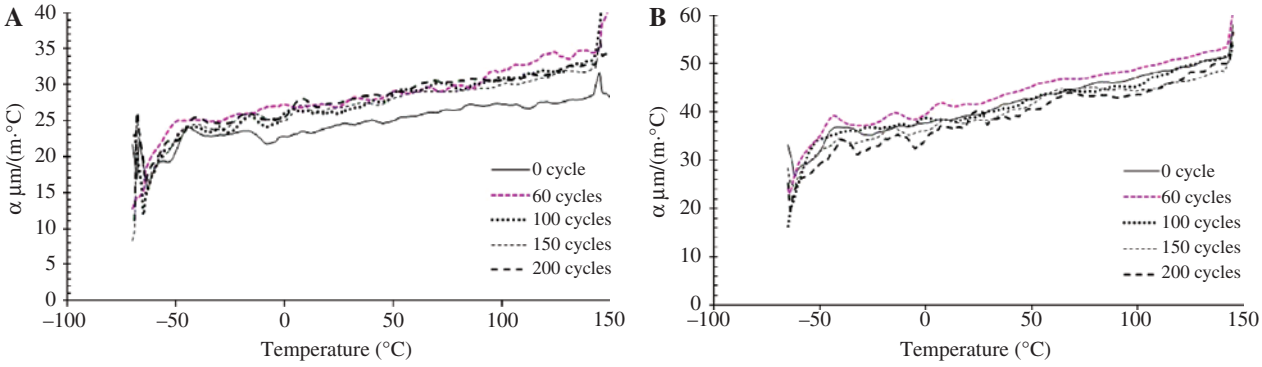

Figure 8: Effect of thermal cycling on through-the-thickness CTE of the (A) UD composite and (B) fabric laminate.

a linear temperature ramp and simultaneously the sample expansion or contraction is monitored and recorded by the probe. During the tests, the machine chamber was cooled from RT to –70°C, and then heated to +150°C and back to RT again, with the heating and cooling rate of 5°C/min. Also, a 10-min dwell time at either temperature extreme (–70°C and +150°C) was done to allow thermal equilibrium to be attained. Five test coupons per laminate were used to measure the CTE. The samples were cut from different areas of the plate in 5×10-mm dimensions.

Figure 8 shows the CTE variation of both the UD and fabric composites with different numbers of thermal cycles. The CTE of the cross-ply fabric is higher than that of the UD laminate. It can be attributed to the higher resin content in the cross-ply fabric laminates (36 wt%) compared to the UD laminate (33 wt%). For a better comparison of the results, a polynomial trend line was used to fit to the curve as shown in the inset figure. The CTE of the UD composite, even though it exhibits fluctuations, first jumps to a higher value when exposed to 60 cycles. By increasing the cycles to 100, the CTE decreases to a smaller amount compared with its initial jump. Further cycling up to 200 cycles indicates no significant change in the CTE of the UD composite samples. Thus, thermal cycling caused an increase in through-the-thickness CTE of the UD composite compared with unexposed samples. Similar to the UD laminate, where the CTE jumped for the first 60 cycles, the CTE of the cross-ply fabric first increases. However, unlike the UD laminate, further thermal cycling decreases the CTE to values even lower than the CTE of the unexposed sample.

4 Discussion

Here, the effort is to find the connections between the experimental results and the factors affecting them. Thermal cycling may affect the properties of carbon fiber polymer composites in two different ways: by more cross-linking in the polymer chain due to post-curing and/or by inducing damages due to the CTE mismatch in the form of matrix cracking or fiber/matrix debonding. These two competing factors are briefly explained in the following.

During thermal cycling at high temperatures (particularly close to curing temperature), the temperature rise can induce post-curing to some extent and cause the improvement of cross-linking degrees of the resin matrix [23], which in turn may improve some physical and mechanical properties. Alternatively, during the thermal cycling test, both the fiber and matrix in the composite are frequently exposed to severe temperature changes from –196°C to +140°C, and each of them behaves in a different way. By increasing the temperature, the carbon fiber contracts and the matrix expands due to different CTEs. As a result of thermal cycling, the CTE difference (or CTE mismatch) induces cyclic thermal stresses whose maximum is at –196°C. It should be mentioned that there might be a difference in the CTE between the different plies, particularly for the cross-ply fabric laminate (stacking sequence effect), which generate interlaminar stresses and might cause damages during thermal cycling. Thermal stresses in polymer composites could create microcracks in the polymer and also fiber/matrix debonding, which could simply grow and propagate within the structure which consequently prevents efficient load transfer and lead to damages and change the properties [4, 5, 28, 29]. It should be emphasized that in the matter of competing effect between the cross-linking and the matrix cracking, the whole specimen should be considered and not only its surface. In this research, however, the microscopy was done only on the surface and there was no information on the possible internal damages, if there was any. Mostly, the chance of having cracks in the surface due to the CTE mismatch seems to be higher because the specimens were not confined and could freely and symmetrically expand/contract in all directions.

In terms of void content after curing, both the UD and cross-ply fabric laminates had voids due to the OOA curing of the material and the absence of oven pressure during the cure. In the UD specimens, no visible crack was observed at the early stage of cycling, but a few were identified after 350 thermal cycles (Figure 1). On the contrary, the cross-ply fabric laminate demonstrated several microcracks in the early cycles. Particularly in the cross-ply fabric laminate, the vertical microcracks appeared after only one thermal cycle in the 90° fiber strand near the sample edge (Figure 2). With further cycling, microcrack density in the outer layers increased and then stabilized up to 10 thermal cycles. The microcracks in the inner layers initiated after five thermal cycles. Then, with the increase of the number of thermal cycles up to 40 (Figure 3), the number of inner microcracks also increased and damage continued to progress in the inner layers. No debonding between the fiber and the matrix was observed up to 40 thermal cycles for the cross-ply fabric laminate. All the cracks were vertical around the voids or edges and tended to grow through the whole thickness of the 90° fiber tows, as shown in Figures 2 and 3.

The ILSS of UD and the cross-ply fabric laminates measured by short beam shear tests was affected by thermal cycling in different ways. The ILSS of the UD laminate was not actually influenced by the thermal cycles up to 200 times, while the ILSS of the cross-ply fabric laminate was significantly affected and reduced by ~10%. These results are in agreement with the microscopy observation where vertical cracks were observed in the cross-ply fabric laminate from the first cycle, while no crack (at least on the surface) was observed even after 350 thermal cycles in the UD laminate. Therefore, in the case of the cross-ply fabric laminate, CTE mismatch and internal damages due to induced thermal stresses played a dominant role in competition with post-curing effect such that with the increase of crack density in the cross-ply fabric laminate, its ILSS decreased. Conversely, cross-linking and matrix cracking had an almost equal effect on the UD laminate. Such a trend was also reported by Gao et al. [25], who studied thermal cycling of UD carbon/epoxy composite. They mentioned that this behavior is mainly due to the changes in the shear strength of the epoxy, which would vary with the density of the cross-linking. In the case of the laminates studied in this research, the DSC results showed that the cross-ply fabric laminate reached a higher degree of cure than the UD laminate. Therefore, post-curing during thermal cycling of UD could occur at a greater extent compared with the cross-ply laminate.

The results of the DMA are also in agreement with the ILSS results. The storage modulus (E') of the cross-ply fabric laminate compared with the UD laminate decreased significantly by the increase of the number of thermal cycles. Particularly at RT, $E'_{\text{cross-ply}}$ decreased by ~19% after exposure to 200 thermal cycles, while E'_{UD} decreased less than 3%. Therefore, it is expected that the storage modules at RT and the strength of the material, such as ILSS, are affected in almost the same way by the thermal cycling. Therefore, in the case of the cross-ply fabric laminate, ILSS and storage modulus were both significantly affected by the thermal cycling, which increased the crack density, whereas these properties in the case of the UD laminate are not influenced by the thermal cycling up to 350 cycles (low crack density). These results are also in good agreement with the microscopy results. The fact that E'_{UD} did not change significantly after exposure to 350 thermal cycles indicates that the damage induced to the matrix material was not big enough, which conforms to the microscopy observations. In the same way for the cross-ply fabric laminate, the reduction of storage modulus by the increase of thermal cycles is an indication of an increase in the number of microcracks, which is in agreement with the observations by optical microscopy, where microcracks initiated from early cycles. It is worth mentioning that the change in storage modulus measured by DMA is mainly related to changes in the polymer. The reason for this is that in the three-point bending test of the UD laminate in DMA, fibers are perpendicular to the bending load, and thus, the properties measured by DMA are more related to the structural changes in the polymer matrix [26, 30].

The trend of T_g variation with respect to the number of thermal cycles for UD is different from that of the cross-ply fabric laminate (Figure 7). There was a slight increase of 1.6% in the T_g of the UD laminates after 150 thermal cycles followed by a 7.4% decrease up to 350 cycles. Such a trend, which was already observed by other researchers [4, 5, 25, 31], is believed to be due to the increase in the degree of cross-linking of the resin caused by the temperature rise during first 150 thermal cycles and, consequently, the post-curing effect to some extent. As the thermal cycle increases, it seems that there is not further curing, but probably some internal damages and microcracks due to the CTE mismatch initiated and increased. As a result, the T_g of the UD laminate gradually decreases after 150 cycles. Moreover, the loss modulus values obtained from the DMA tests also confirmed this behavior: insignificant increase during the first 150 cycles, and then continuous increase up to 350 cycles. Unlike the UD laminate, the T_g of the cross-ply laminate had a reduction of 3.6% after 30 cycles followed by an increase of 2.7% after 30 cycles. The initial decrease could be due to the increasing level of crack density, which was also observed in the

microscopy images, whereas the following increase was probably caused by more cross-linking in resins. This is also in agreement with previous results, for example, the storage modulus of the cross-ply laminate reduced due to the increase of the crack density. The peak of tan δ for both the UD and cross-ply laminates decreased by the increase of thermal cycles, which was more significant for the cross-ply laminate. Moreover, the curve at the peak of the cross-ply laminate broadens to a greater extent compared with the UD laminate. This indicates that stiffness increased while viscosity decreased, which probably is due to the decreased mobility of the molecular chain. As the polymer was under thermal cycling at high temperature close to its T_g, additional cross-linking and post-curing occurred, which consequently caused an increase in T_g [27].

CTE is dependent on the temperature and is also affected by thermal cycling. For both UD and cross-ply laminates, CTE through-the-thickness was positive and increased with increasing temperature. It should be remembered that the CTE of carbon fibers in the transverse and longitudinal directions is positive and negative, respectively, and the polymer CTE is positive in all directions. Therefore, for carbon fiber-reinforced composites, lamina CTE could be negative in the fiber direction, but positive in the transverse direction. Moreover, in the transverse direction, CTE is matrix dominant. In the case of the UD laminate, the CTE jumped to a higher value when exposed to 60 cycles (about 13% higher at RT) followed by a slight decrease compared with its initial jump by further cycling to 200 cycles. Thus, thermal cycling caused an increase in CTE through-the-thickness of the UD laminate in a wide range of temperature. This increase became more significant at higher temperatures. The CTE of the cross-ply fabric laminate first increased during the first 60 cycles, similar to the CTE of the UD laminate; however, further thermal cycling decreased its CTE even lower than the CTE of the unexposed sample. The first increase could be explained by the post-curing as the fabric laminate was not fully cured. As observed by the microscopy, further cycling increased the crack density of the matrix, which resulted in the loss of the matrix integrity and, consequently, CTE reduction, which was also reported by other researchers [5, 32].

5 Conclusions

In this study, the effects of thermal cycling on the mechanical and thermal properties of flat laminates made of OOA carbon/epoxy prepregs were examined. The study was conducted on both UD tape laminates and cross-ply 5HS fabric laminates of the same thickness, exposed to different number of thermal cycles (30–350 cycles) in a temperature range from –196°C to +140°C. Several experimental testings were conducted to characterize the different mechanical and thermal properties, and the main affecting factors influencing these properties were identified. It was found that the variation of different properties due to the thermal cycling could be described by a competing effect between two main factors: (i) more cross-linking in the polymer chain and post-curing due to the temperature rise in thermal cycles; (ii) induced damages in the form of matrix cracking or fiber/matrix debonding due to the CTE mismatch. Optical microscopy observation revealed that very little crack was initiated in the UD laminate even after 350 thermal cycles. However, for the cross-ply fabric laminate, several microcracks were detected even at the early stage of cycling. All the cracks in the cross-ply laminate were vertical (through-the-thickness) around the voids or edges (no debonding). It was observed that the presence of the void can have an impact on the initiation and propagation of microcracks. The size of the void can determine the timing of microcrack initiation and propagation. Larger voids cause microcracks to form earlier during thermal cycling.

Acknowledgments: The authors would like to acknowledge the financial support from the Natural Sciences and Engineering Research Council of Canada, the Consortium De Recherche Et D'innovation En Aérospatiale Au Québec, MDA Corporation and Stelia North America.

References

[1] Rawal SP, Goodman JW. In *Comprehensive Composite Materials*, Kelly, A, Zweben, C, Eds., Elsevier: Amsterdam, 2000, pp 279–315.
[2] Han J, Kim C. *Compos. Struct.* 2006, 72, 218–226.
[3] George P, Dursch H. *J. Adv. Mater.* 1994, 25, 10–19.
[4] Han J, Qin Y, Gao W, Sun M. In *Proceedings of the International Astronautical Congress*, *IAC*, 2014, pp 5859–5866.
[5] Yu Q, Chen P, Gao Y, Mu J, Chen Y, Lu C, Liu D. *Mater. Chem. Phys.* 2011, 130, 1046–1053.
[6] Sanborn J, Morel D. *J. Reinf. Plast. Compos.* 1988, 7, 155–164.
[7] Henaff-Gardin C, Lafarie-Frenot M. *Int. J. Fatigue* 2002, 24, 171–177.
[8] Shimokawa T, Katoh H, Hamaguchi Y, Sanbongi S, Mizuno H, Nakamura H, Asagumo R, Tamura H. *J. Compos. Mater.* 2002, 36, 885–895.
[9] Herakovich CT, Hyer M. *Eng. Fract. Mech.* 1986, 25, 779–791.
[10] Henaff-Gardin C, Lafarie-Frenot M, Gamby D. *Compos. Struct.* 1996, 36, 113–130.

[11] Adams DS, Bowles DE, Herakovich CT. *J. Reinf. Plast. Compos.* 1986, 5, 152–169.
[12] Bechel VT, Camping JD, Kim RY. *Compos. B Eng.* 2005, 36, 171–182.
[13] Bechel VT, Kim RY. *Compos. Sci. Technol.* 2004, 64, 1773–1784.
[14] Bechel VT, Fredin MB, Donaldson SL, Kim RY, Camping JD. *Compos. Part A Appl. Sci. Manuf.* 2003, 34, 663–672.
[15] Timmerman JF, Tillman MS, Hayes BS, Seferis JC. *Compos. Part A Appl. Sci. Manuf.* 2002, 33, 323–329.
[16] Kessler SS, Matuszeski T, McManus H. In *Proceedings of the American Society for Composites*, Blacksburg, VA, 2001, pp 93–111.
[17] Ajaja J, Barthelat F. *Compos. B Eng.* 2016, 90, 523–529.
[18] Tompkins SS. In *NASA (SDIO) Space Environmental Effects on Materials Workshop, Part 2*, US, 1989, pp 447–470.
[19] Shanker A, Sullivan RW, Drake DA. In *Composite, Hybrid, and Multifunctional Materials*, Springer: Amsterdam, 2015, Vol. 4, pp 29–37.
[20] Jackson K, Crabtree M. Autoclave quality composites tooling for composite from vacuum bag only processing, presented at the *47th International SAMPE Symposium and Exhibition*, Long Beach, CA, USA, 2002, pp 800–807.
[21] Grimsley BW, Sutter JK, Dixon GD, Smeltzer SS. *NASA Langley Research Center, Hampton, VA, United States*, 2013.
[22] Sutter JK, Kenner WS, Pelham L, Miller SG, Polis DL, Nailadi C, Hou T-H, Quade DJ, Lerch BA, Lort RD, Zimmerman TJ, Walker J, Fikes J. *Elevated Temperature, Notched Compression Performance of Out of Autoclave Processed Composites*, NASA Langley Research Center, Hampton, VA, 2010.
[23] Cauberghs J. *Out-of-Autoclave Manufacturing of Aerospace Representative Parts*, Master thesis, Mechanical Engineering Department, McGill University, Montreal, Quebec, 2011.
[24] (October 2015). *cycom® 5320-1 epoxy resin system technical data sheet*.
[25] Gao Y, He S, Yang D, Liu Y, Li Z. *Compos. B Eng.* 2005, 36, 351–358.
[26] Bosze EJ, Alawar A, Bertschger O, Tsai Y-I, Nutt SR. *Compos. Sci. Technol.* 2006, 66, 1963–1969.
[27] Goertzen WK, Kessler MR. *Compos. B Eng.* 2007, 38, 1–9.
[28] Parlevliet PP, Bersee HE, Beukers A. *Compos. Part A Appl. Sci. Manuf.* 2006, 37, 1847–1857.
[29] Timmerman JF, Seferis JC. *J. Appl. Polym. Sci.* 2004, 91, 1104–1110.
[30] Akay M. *Compos. Sci. Technol.* 1993, 47, 419–423.
[31] Wolff EG. *Metal Progress*, 1979, 115, 54–63.
[32] Shin K, Kim C-G, Hong C-S, Lee H-H. *Compos. B Eng.* 2000, 31, 223–235.